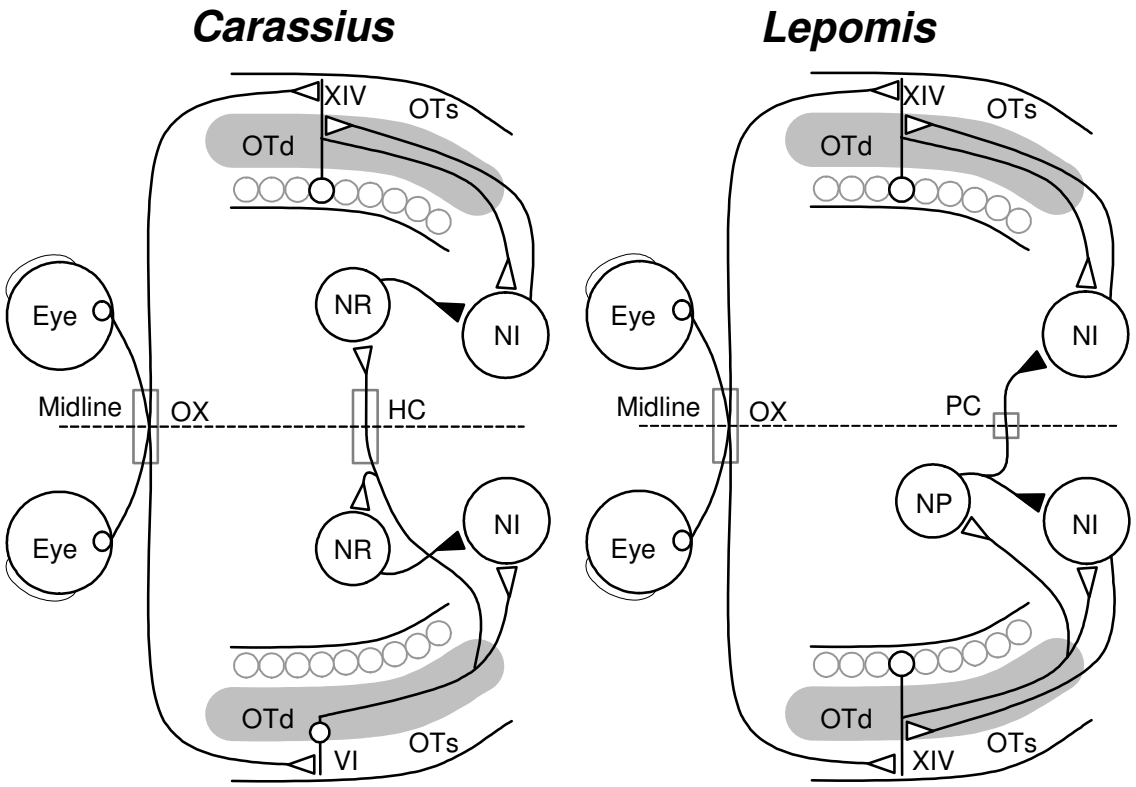

Figure 1. Schematic of tectum-NI connections. Principal nuclei and connections of *Carassius* and *Lepomis* discussed in the text. For more detail see Xue et al., (2001), Striedter and Northcutt, (1989), King and Schmidt, (1993). Open triangles indicate presumed excitatory synapses, filled triangles presumed inhibitory synapses (Ito et al., 1982; King and Schmidt, 1993). Tectal cells (VI and XIV, Meek and Schellart, 1978) of *Carassius* and NP of *Lepomis* are depicted only unilaterally for clarity.

HC	horizontal commissure
NI	nucleus isthmi
NP	nucleus pretectalis
NR	nucleus ruber; the lateral thalamic nucleus (Braford & Northcutt ,1983; King & Schmidt, 1993)
OTd	deep optic tectum
OTs	superficial optic tectum
OX	optic chiasm
PC	posterior commissure
XIV	type XIV pyriform cell
VI	type VI bipolar cell

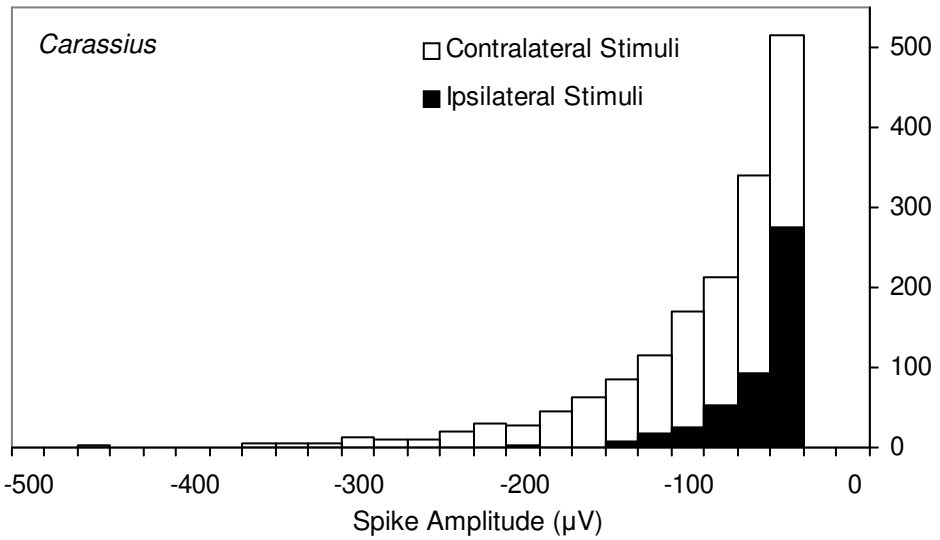

Figure 2. Histograms of spike amplitudes recorded in nucleus isthmi of *Carassius* evoked by ipsilateral and contralateral eye stimuli. Stimuli were 100 msec LED flashes centered in the fields of the contralateral or ipsilateral eyes. Spikes were counted during the 100 msec stimulus and recorded from the core of the nucleus where spikes were mainly negative-going. Results of 20 ipsilateral and 20 contralateral stimulus presentations from two fish.

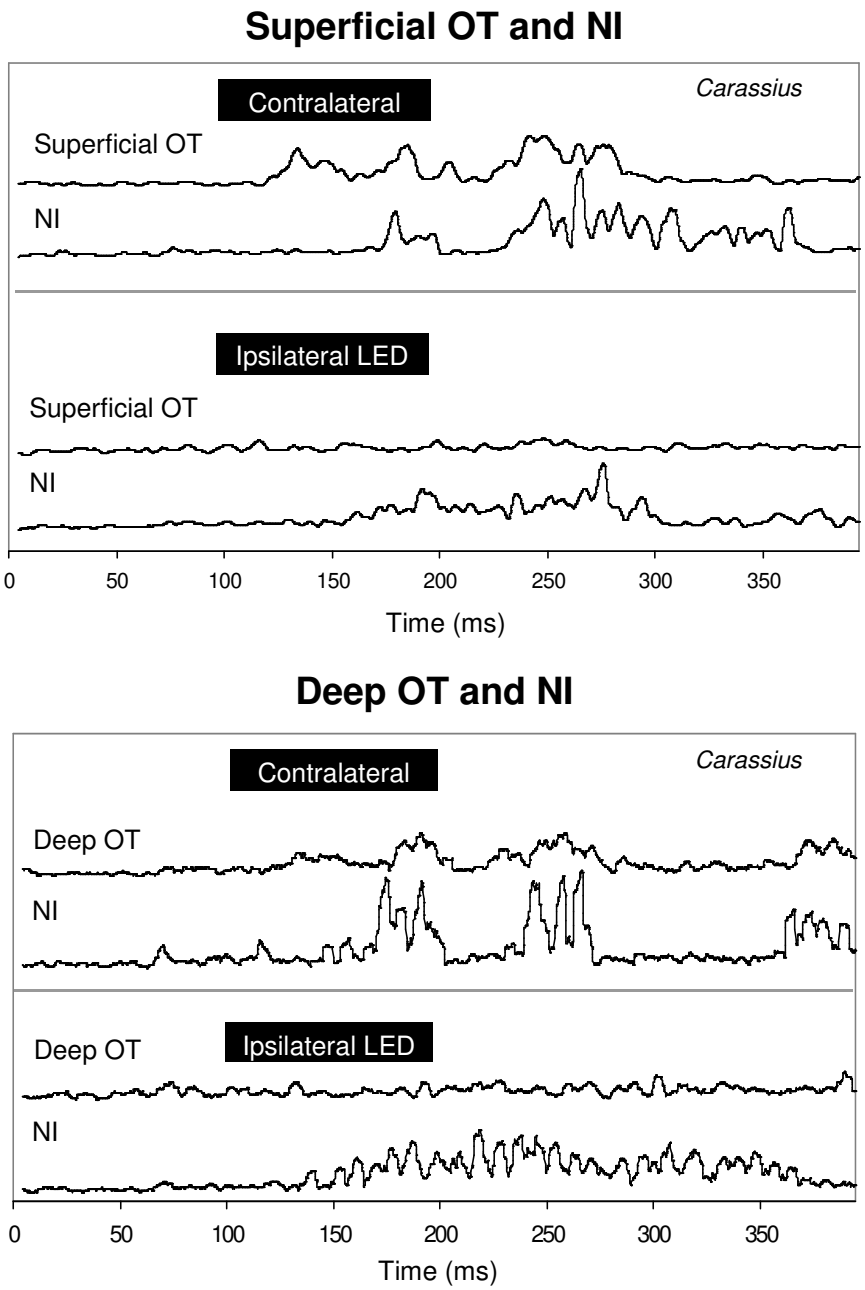

Figure 3. Samples of integrated activity during stimulation with 100 ms LED flashes in the ipsilateral and contralateral fields of *Carassius*. (Top) Simultaneous records from Superficial OT and NI. (Bottom) Simultaneous records from Deep OT and NI.

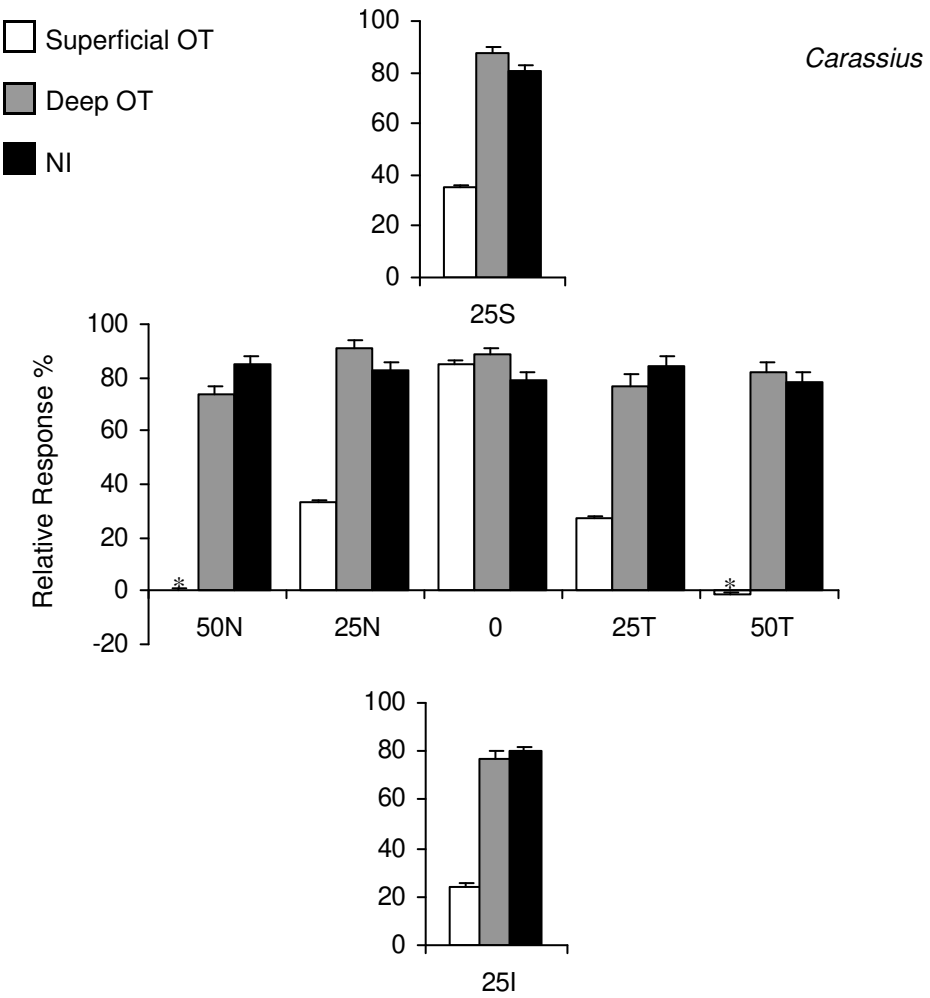

Figure 4. Amplitude of integrated activity recorded from superficial tectum, deep tectum, and nucleus isthmi of *Carassius* in response to 100 ms LED flashes in different parts of the contralateral visual field. Ten responses were recorded from each of seven stimulus positions in five fish. Labels indicate LED positions in degrees relative to the center of the LED array (N nasal, T temporal, S superior, I inferior). Mean responses recorded from superficial OT varied as a function of LED position ($P < 0.01$), whereas those recorded from deep OT and NI did not. Mean responses recorded from deep OT and NI were greater than 0 for all tested LED positions. Mean responses recorded from superficial OT were only significant for stimuli within 25 degrees of the visual axis.
* = no response ($P < 0.01$)

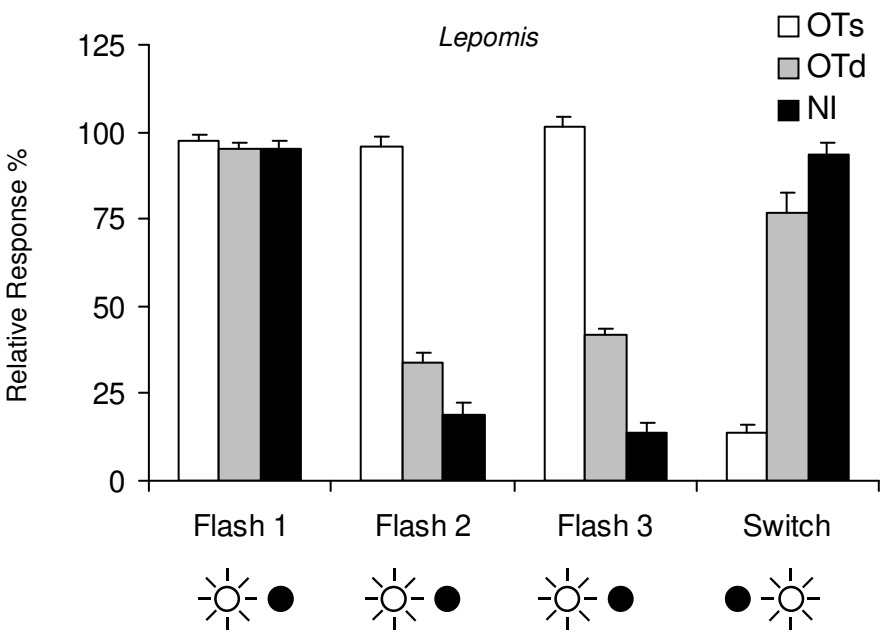

Figure 5. Visual response habituation. Mean response amplitudes (+SEM) recorded from OTs, OTd, and NI of *Lepomis* in response to four consecutive 100 ms LED flashes presented at 60s intervals. Flashes 1-3 were in the center of the OTs multiunit receptive field; the fourth flash (Switch) was 25 degrees from the original location. Mean responses recorded from OTd and NI varied as a function of flash sequence ($P < 0.01$), whereas those recorded from superficial OT did not. OTd and NI habituated to repeated stimulation at the same location, but recovered when the location was changed. The mean NI response to the fourth flash did not differ significantly from the mean response to the first flash ($P > 0.5$). Each bar is the average of 10 responses from 3 individual *Lepomis*. Very similar results were obtained with *Carassius*.

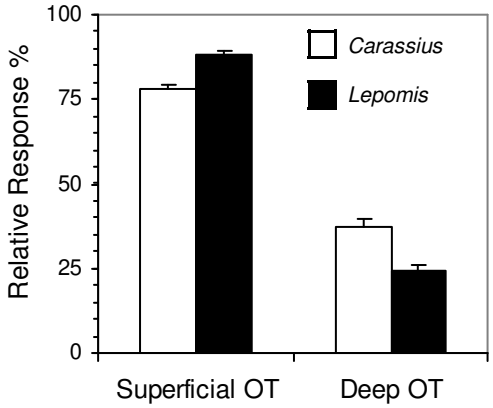

Figure 6. Comparison of stimulus evoked response amplitudes in superficial and deep optic tectum. Mean amplitudes of integrated multiunit bursts (+SEM) recorded in response to a 100 ms LED flash in the center of the tectal receptive field. Mean responses recorded from superficial OT were greater than those recorded from deep OT for each species ($P < 0.01$). Each mean was calculated from 50 responses (10 x 5 animals).

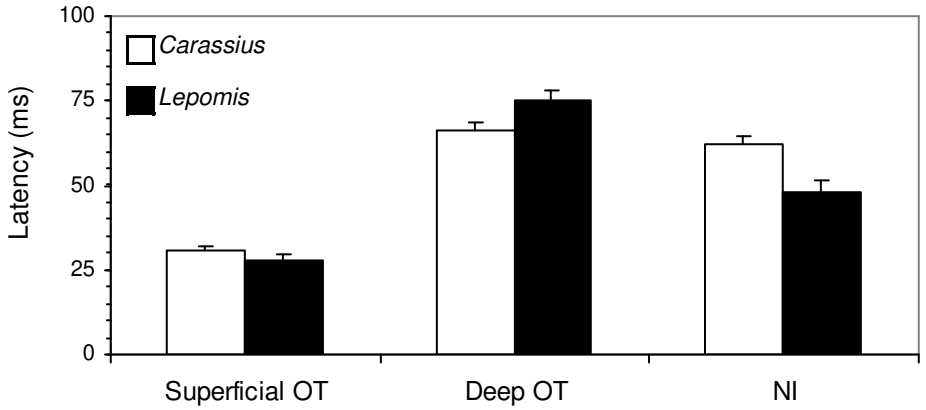

Figure 7. Average response latencies (+SEM) of integrated activity recorded from superficial OT, deep OT, and NI in response to a 100 ms LED flash in the visual field of the contralateral eye. Latencies for each location varied significantly within species with the exception of deep OT and NI of *Carassius* ($P > 0.05$). Each mean was calculated from 50 responses (10 x 5 animals).

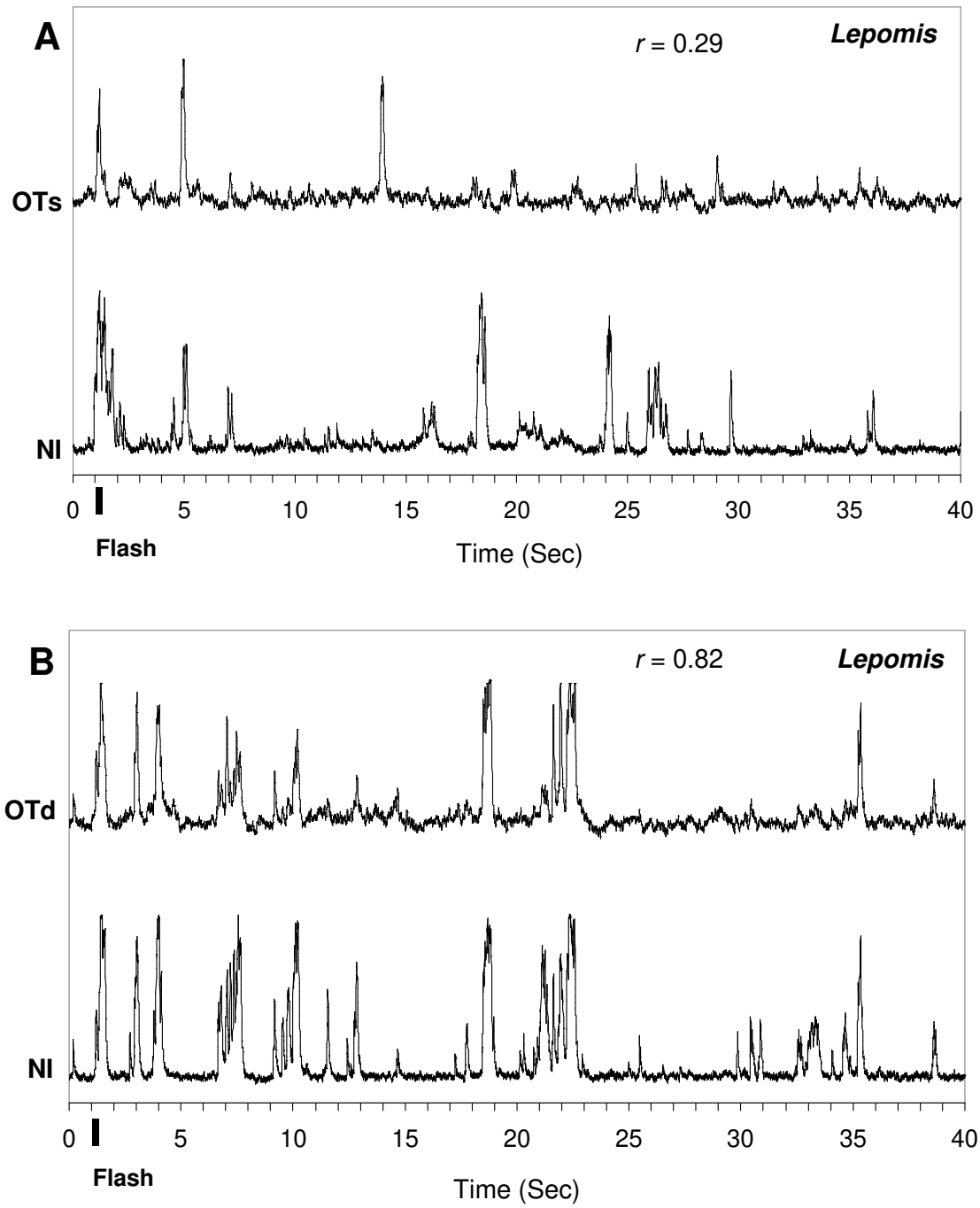

Figure 8. Integrated activity recorded simultaneously in *Lepomis*, **A** from superficial OT (OTs) and NI, and **B** from deep OT (OTd) and NI. A single 200 ms LED flash was presented at T= 1.0 second. Correlation coefficients calculated over the entire 40s given by ***r***.

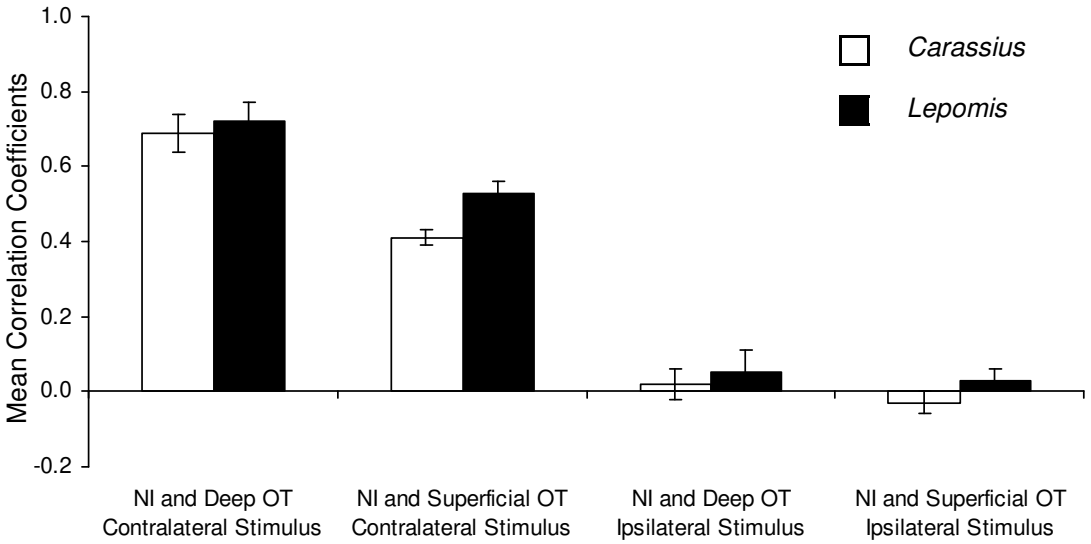

Figure 9. Correlations between activity in OT and NI evoked by contra– and ipsilateral stimulation. Correlation coefficients were calculated from pairs of records similar to those in Fig. 2, using 300 ms of data starting at LED onset. Each bar shows mean correlation coefficients of 10 record pairs from 5 fish of both species. The LED stimulus was presented to the contralateral or the ipsilateral eye.

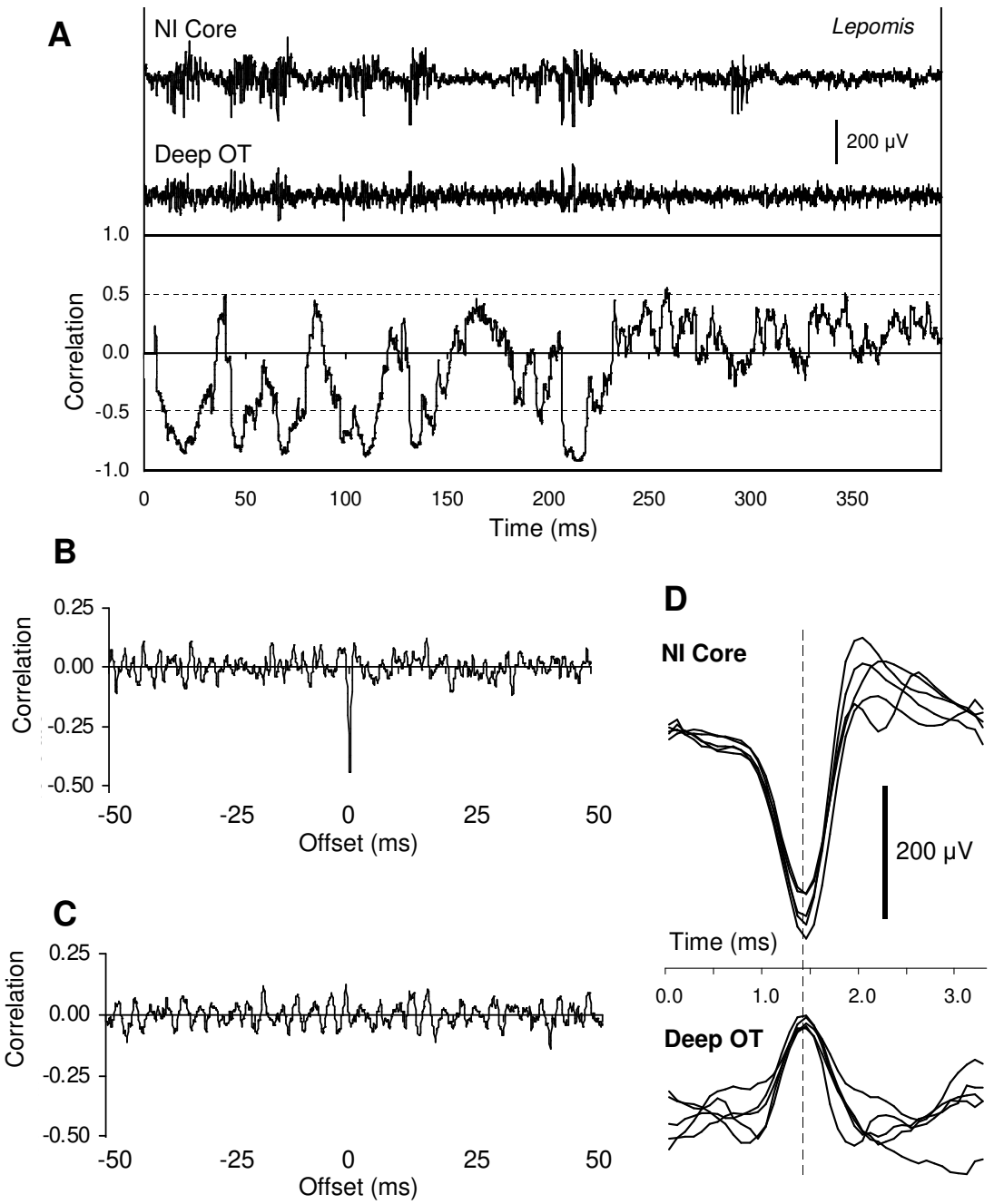

Figure 10. Synchronization of spikes in nucleus isthmi core and deep optic tectum. (A) Spontaneous activity from the core of nucleus isthmi (NI) and deep optic tectum (OT) of *Lepomis*, with a continuous plot of the correlation between the records (5 ms window). (B) Cross correlogram of the records in A. (C) Control correlogram calculated from two nonsimultaneous records. (D) Superimposed records of five negative potentials recorded from the core of NI and five coincident positive potentials recorded from deep OT. Waveforms sampled at 12 kHz.

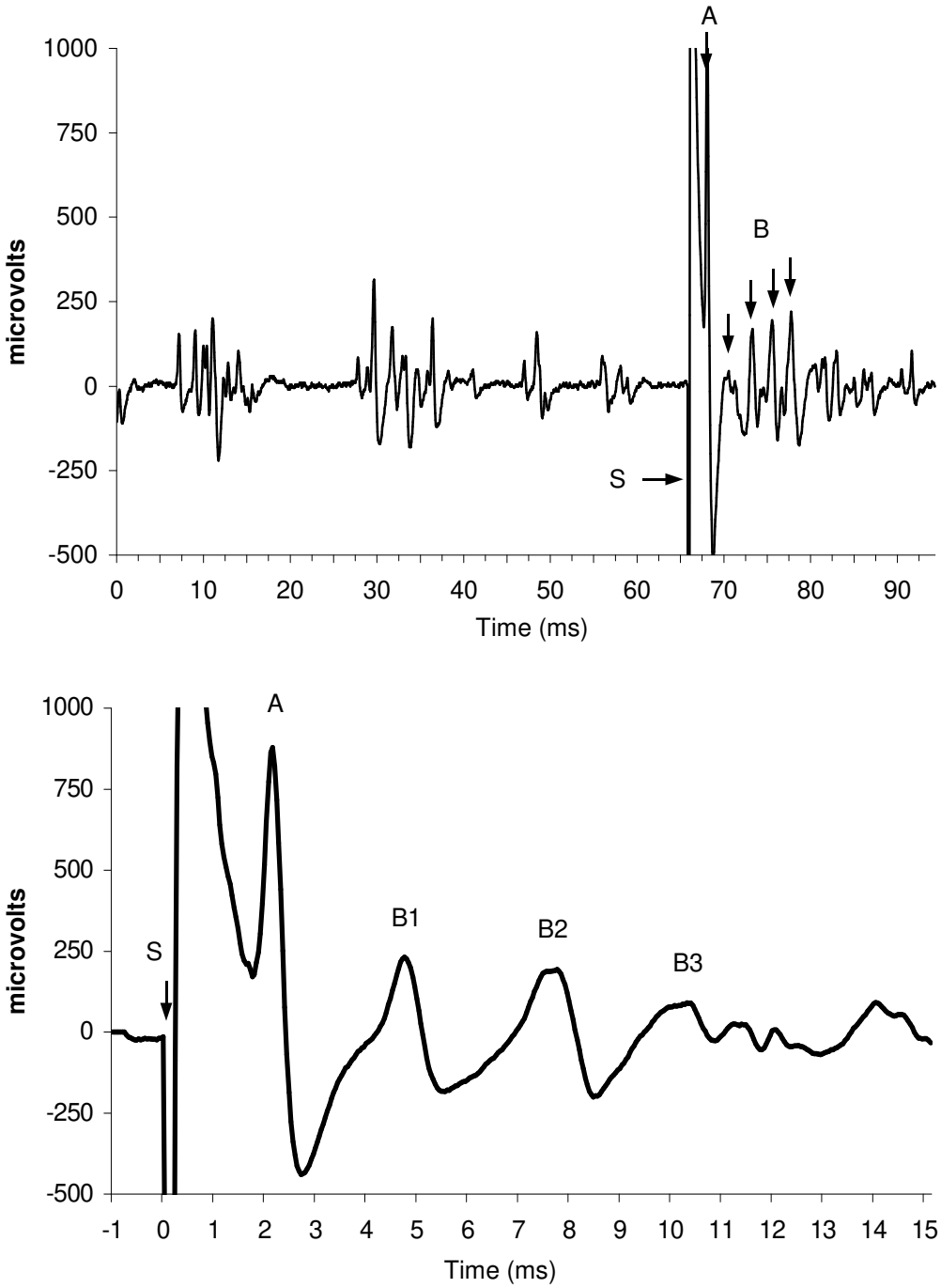

Figure 11. Top: Extracellular potentials recorded from the shell of NI in *Lepomis*. The record initially shows spontaneous bursting activity followed at 65 ms by a single 10 μs electric shock to tectum. This evoked a large, short latency antidromic spike (A) and 4 orthodromically driven potentials (B). Bottom: Average of five NI responses evoked by shocks to tectum showing antidromic (A) and orthodromic potentials (B1-B3) as described by Williams et al. (1983).

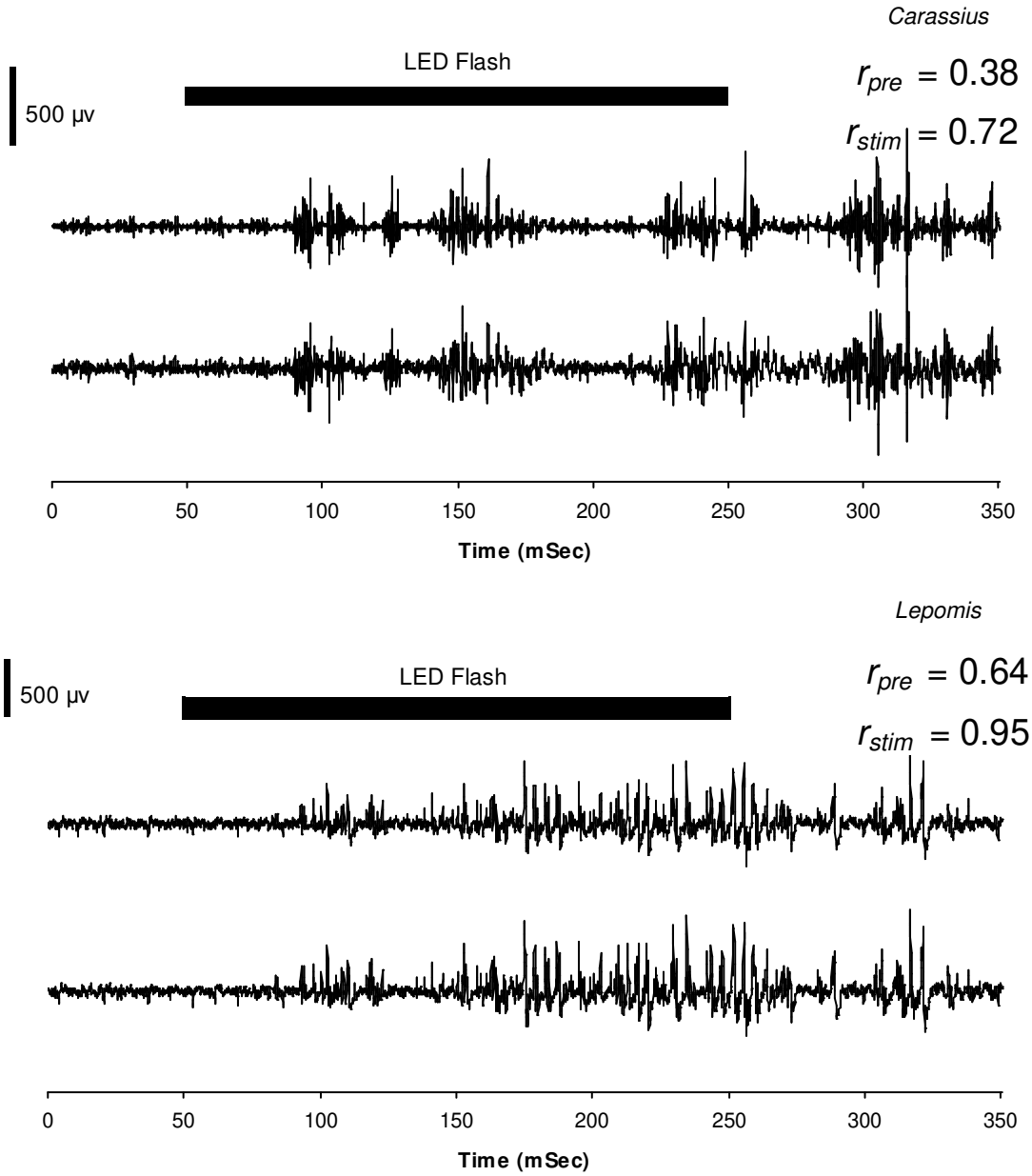

Figure 12. Stereotrode records from nucleus isthmi. Two stereotrode recordings taken from the nucleus isthmi neuropil shell of *Carassius* (top) and *Lepomis* (bottom). The solid bar above each pair of records represents a 200 ms LED flash occurring in the visual field contralateral to the nucleus. The records illustrate the nearly identical traces recorded from two locations separated by approximately 100 µm in the shell of nucleus isthmi. Correlation coefficients for the 50 ms preceding the LED flash (r_{pre}) and for the 200 ms stimulus period (r_{stim}) are displayed for each pair of records.

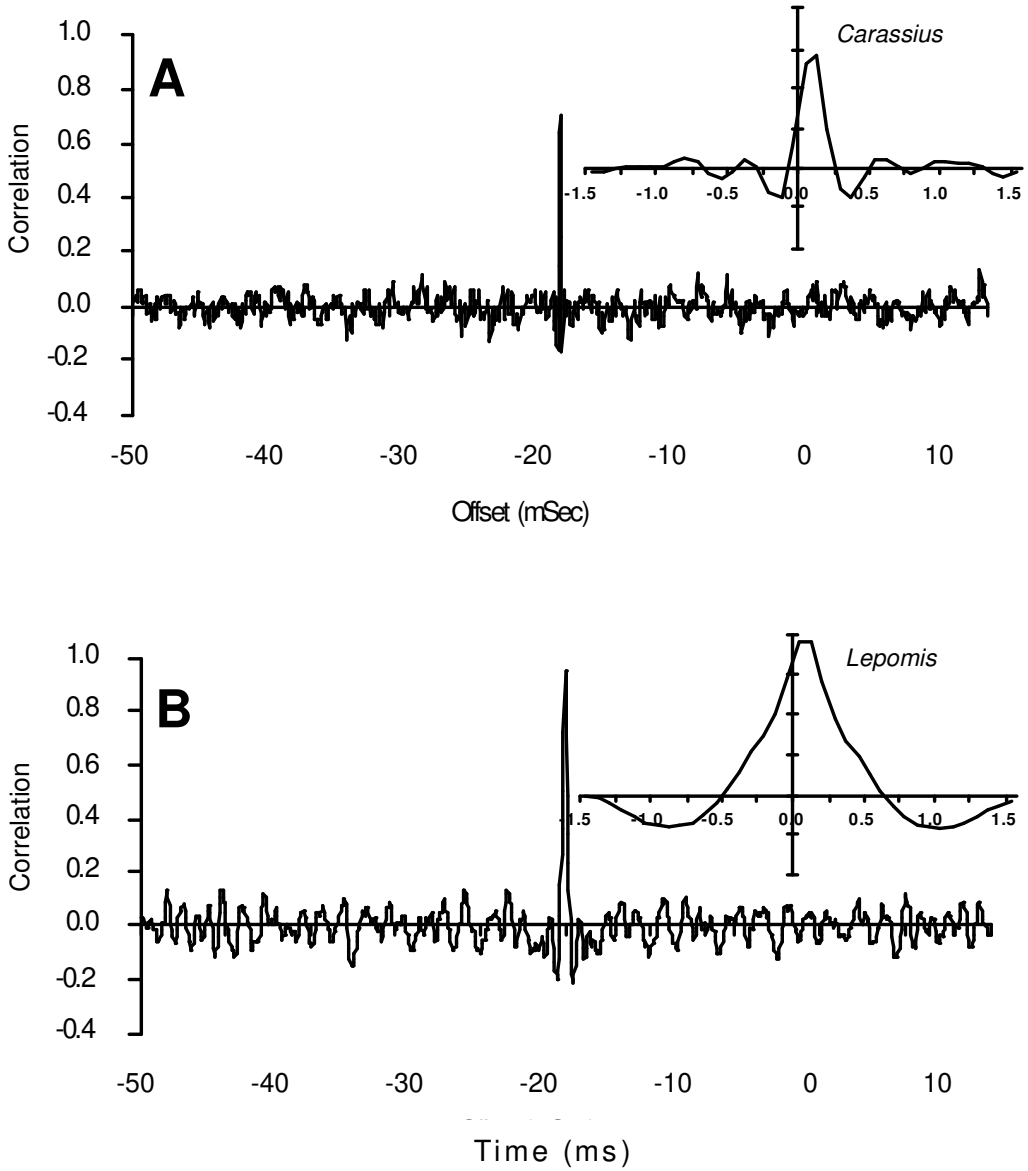

Figure 13. Cross-correlations of recordings made with a stereotrode pair in the shell of NI in *Carassius* (A) and *Lepomis* (B). The insets illustrate high-resolution views of each cross correlogram.